ACS APPLIED MATERIALS & INTERFACES

Research Article

www.acsami.org

Permittivity of Dielectric Composite Materials Comprising Graphene Nanoribbons. The Effect of Nanostructure

Ayrat Dimiev,[†] Dante Zakhidov,[†] Bostjan Genorio,[†,‡] Korede Oladimeji,[§] Benjamin Crowgey,[§] Leo Kempel,*[,§] Edward J. Rothwell,*[,§] and James M. Tour*[,†,⊥,∥]

[†]Department of Chemistry, [⊥]Department of Mechanical Engineering and Materials Science, and [∥]Smalley Institute for Nanoscale Science and Technology, Rice University, MS-222, 6100 Main Street, Houston, Texas 77005, United States

[‡]Faculty of Chemistry and Chemical Technology, University of Ljubljana, Aškerčeva cesta 5, 1000 Ljubljana, Slovenia

[§]Department of Electrical and Computer Engineering, Michigan State University, East Lansing, Michigan 48824, United States

Supporting Information

ABSTRACT: New lightweight, flexible dielectric composite materials were fabricated by the incorporation of several new carbon nanostructures into a dielectric host matrix. Both the permittivity and loss tangent values of the resulting composites were widely altered by varying the type and content of the conductive filler. The dielectric constant was tuned from moderate to very high values, while the corresponding loss tangent changed from ultralow to extremely high. The data exemplify that nanoscale changes in the structure of the conductive filler result in dramatic changes in the dielectric properties of composites. A microcapacitor model most explains the behavior of the dielectric composites.

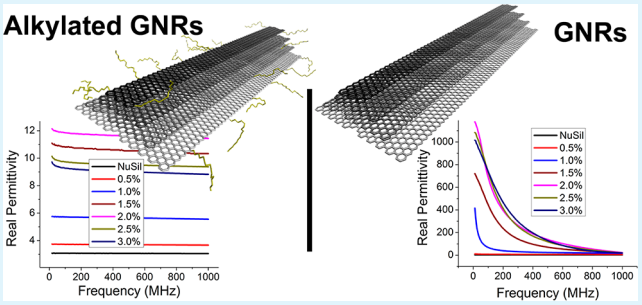

KEYWORDS: *dielectric composite, permittivity, loss tangent, graphene nanoribbons*

INTRODUCTION

Composite materials comprising conductive fillers in a dielectric host gained significant attention recently for their potential in electronic engineering. Carbon nanotubes (CNTs) have been used extensively as the conductive filler because of their ability to interact strongly with impressed radio and microwave fields.[1−5] The incorporation of CNTs into a dielectric polymer matrix significantly increases the dielectric constant of the resulting composite material.[3−8] Because of their high aspect ratio and high persistence length based on their tubular rigidity, only very low weight fractions of CNTs are required to significantly increase the permittivity of a polymer. The incorporation of CNTs increases both the real and imaginary parts of permittivity, and the resulting composites exhibit very high loss even at fractions as low as 0.5 wt %.[5,6,8] At the same time, miniaturization of electronic components requires materials with high permittivity and low loss in the radio and low-frequency microwave regions.[9] In the high-frequency microwave region, low loss is critical for antennas. High-loss materials, in turn, have potential applications for electromagnetic shielding and technologies that reduce the reflection coefficient from the objects. From the perspective of fabricating composite materials, multiwalled CNTs (MWCNTs) have higher potential compared to single-walled CNTs (SWCNTs) because of their higher performance-to-price ratio.

The physics behind the electromagnetic behavior of composites remains elusive. The major approach currently used to explain the permittivity of composite materials is percolation theory. Percolation theory[10−13] predicts a power-law behavior of composites. The dependence of the dielectric constant on the fraction of conductive filler (filling fraction) is expressed by eq 1

$$\varepsilon = \varepsilon_h |(f_c - f)/f_c|^{-q} \quad (1)$$

where f is the volume fraction of conductive filler, f_c is the percolation threshold, and q is the critical exponent. According to eq 1, the dielectric constant can reach extremely high values in the vicinity of the percolation threshold, where $f \rightarrow f_c$. A power dependence of the dielectric constant on the frequency (ω) can be expressed according to eq 2[14]

$$\varepsilon' = \varepsilon_h + A\omega^{-x}; \quad \varepsilon'' = B\omega^{-y} \quad (2)$$

where ε' and ε'' are the real and imaginary parts of the complex permittivity ($\varepsilon = \varepsilon' + i\varepsilon''$) of the composite, ε_h is the permittivity of the dielectric host, A and B are the proportionality coefficients, and x and y are the so-called "critical exponents". In percolation theory, critical exponents are considered to be "universal", or independent of the type of

Received: May 16, 2013
Accepted: July 15, 2013
Published: July 15, 2013

composite and filler. Percolation theory explains the macroelectronic properties of composites by statistical distribution of clusters and neglects the role of the nature of the dielectric host and conductive filler. Although this approach has garnered significant interest, experiments poorly support the universality of the power laws. Thus, the critical exponents obtained by fitting experimental results to eqs 1 and 2 vary significantly,[13−18] and while the percolation threshold was confirmed in several experiments, no percolating behavior was observed in many others.

In addition to percolation theory, a microcapacitor model is employed to explain the electronic properties of dielectric composites.[17−19] According to this model, the composite material is considered to be a network of microcapacitors randomly distributed in a dielectric host. We show here that the microcapacitor model better explains our experimental results. Regardless of the complementary approaches of percolation theory and the microcapacitor model, the precise physical behavior of composite materials remains poorly understood.

In our group, we have recently prepared several carbon nanostructures that can be used as conductive fillers in dielectric composites. The incorporation of these nanostructures allows us to alter the macroscopic properties of composites over a wide range. Here we investigate the fundamental science of nanoscopic changes in the conductive filler structure affecting the macroscopic dielectric parameters of composite materials.

A two-part silicone elastomer (NuSil Technology R-2615) was used as the host polymer becaise of its light weight, high flexibility, excellent mechanical properties, and ease of tailoring shapes through simple cutting with scissors or a razor blade. The samples were tested in the 1−1000 MHz spectrum by the impedance method. The precise determination of the volume fractions of the conductive filler in composites is difficult because the density of carbon nanostructures is variable depending on structure. Here we have listed the weight percentage of the conductive filler unless otherwise specified.

EXPERIMENTAL SECTION

The MWCNTs were provided by Mitsui and Co. and were used without further treatment.

Preparation of Carbon Nanostructures. The K-split MWCNTs, K/Na-unzipped graphene nanoribbons (GNRs), and hexadecyl GNRs (HD-GNRs) were prepared as we described previously.[20,21]

K-Split MWCNTs. These were prepared as previously published but with different amounts for the work here.[20,22] "MWCNTs (1.00 g) and potassium metal pieces (3.00 g) were placed in a 50 mL Pyrex ampoule. The ampoule was evacuated and sealed with a flame." ***Caution!*** *All synthetic steps involving Na/K alloy should be carried out with extreme caution under strict exclusion of air and moisture, under inert gas, and appropriate personal protection (hood, blast shields, face shield, protective and fire resistant clothing) should be used at all times.* "The ampoule was heated in a furnace at 250 °C for 14 h. The heated ampoule, containing a golden-bronze-colored potassium intercalation compound, was cooled to room temperature, opened in a glove box, and mixed with 20 mL of Et_2O. Next, 20 mL of EtOH was slowly added into the reaction mixture. After removal from the drybox, the quenched product was washed consecutively with EtOH, H_2O, and Et_2O and filtered through a 0.40 μm PTFE (Teflon) membrane. The as-prepared K-split MWCNTs were characterized and used to make composite materials."

K/Na-Unzipped GNRs. These were prepared as previously published but with different amounts for the work here.[21] "A sample of MWCNTs (100 mg, 8.3 mmol) was added to an oven-dried 250 mL round-bottom flask containing a magnetic stir bar. The vessel was then transferred to a N_2 glove box where freshly distilled 1,2-dimethoxyethane (35 mL) and liquid Na/K alloy (0.29 mL) were added." ***Caution!*** *All synthetic steps involving Na/K alloy should be carried out with extreme caution under strict exclusion of air and moisture, under inert gas, and appropriate personal protection (hood, blast shields, face shield, protective and fire resistant clothing) should be used at all times.* "The suspension was then sealed with a septum and transferred out of the glove box where it was dispersed by a short 5 min ultrasonication (using ultrasonic cleaner Cole-Parmer model 08849-00) to yield a dark greenish to red suspension. After ultrasonication, the reaction mixture was vigorously stirred (450 rpm) at room temperature for 24 h. The reductive unzipping of the MWCNTs can be followed visually by the color change of the reaction mixture as it became a finely dispersed green or red suspension. The reaction suspension was then quenched by the addition of methanol (20 mL, 500 mmol) using a syringe, and the mixture was then allowed to stir at room temperature for 10 min. For workup, the reaction mixture was filtered over a PTFE membrane with a 0.45 μm pore size. The remaining solid was successively washed with THF (100 mL), *i*-PrOH (100 mL), H_2O (100 mL), *i*-PrOH (20 mL), THF (20 mL), Et_2O (10 mL) and dried under vacuum at 60 °C for 24 h."

HD-GNRs. To prepare HD-GNRs, to the reaction mixture of K/Na-unzipped GNRs, prepared as described above, was injected 1-iodohexadecane (1.20 g, 3.41 mmol) in 10 mL of dimethyl ether, and the reaction mixture was stirred for 24 h at 60 rpm. To quench any active species that remained, the reaction mixture was treated with methanol. Crude functionalized HD-GNRs were collected by filtration using a 0.2 μm PTFE membrane and then subjected to a thorough workup procedure including several washings with organic solvents and water as described above for the K/Na-unzipped GNRs. Before analysis, all of the products were dried under vacuum at 60 °C for 24 h.

Production of Composite Materials. The composite materials were made using a two-part silicon elastomer (NuSil Technology R-2615, NuSil), as we described earlier.[22] "The conductive filler (MWCNT or GNR from 6.0 mg to 36.0 mg depending on the loading) was sonicated (Cole Palmer ultrasonic cleaner B3-R) for 2 min in 10 mL of chloroform to obtain a suspension. The contents of the conductive filler are weight percentages. Separately, part A of NuSil (1.08 g) was dissolved in 10 mL of chloroform. The GNR−chloroform suspension was added to the elastomer solution and the mixture was stirred. The resulting mixture was left in the hood under a slow blowing flow of air at room temperature for 12−18 h to permit most of the chloroform to evaporate. This sequence of blending and solvent evaporation facilitated uniform dispersion of the GNRs in the polymer matrix. Such a high level of dispersion was not achieved by simple mechanical blending of GNRs into the NuSil. Next, the mixture was placed in a vacuum oven (10 mm Hg, 60 °C) for 2 h to remove the remaining chloroform. Part B of the NuSil elastomer (0.12 g) was added into the mixture and manually stirred 2−3 min to mix parts A and B. The mixture was then poured into the bottom part of an appropriately shaped (see below) mold, and was placed into an evacuated desiccator for 30 min to remove trapped air. The top of the mold was then placed atop and the elastomer was cured in an oven in the air at 100 °C for 3 h."

Electrical Measurements. "The permittivity and loss values were calculated from capacitance values measured with an impedance analyzer (Agilent E4991A RF). The samples were cylindrical with a diameter of 20.0 mm and the height (thickness) of 2.0 mm. To reduce the measurement uncertainty, five scans were recorded for every sample, and the average values are reported below."[22]

RESULTS AND DISCUSSION

Three different types of carbon nanostructures were used in this work as conductive fillers. Figure 1 shows the structure and morphology of all three types along with those of the parent MWCNTs (Figure 1a). The first type of conductive filler was prepared by potassium vapor splitting of MWCNTs (K-split MWCNT).[20] As-prepared K-split MWCNTs (Figure 1B)

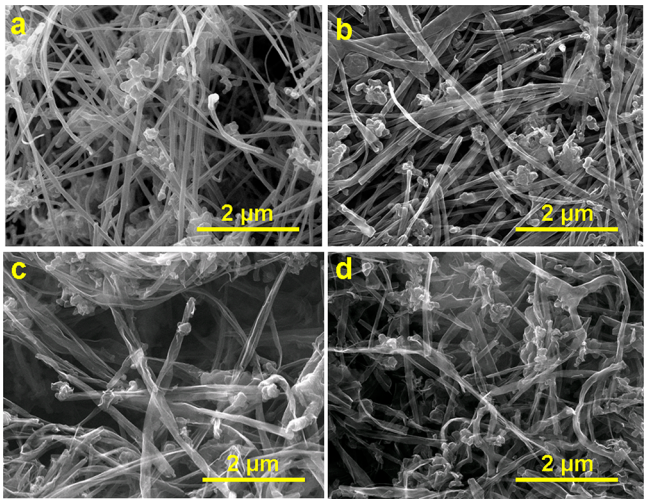

Figure 1. SEM images of different types of carbon nanostructures: (a) original MWCNTs; (b) K-split MWCNTs; (c) K/Na-unz GNRs; (d) HD-GNRs.

appear to be somewhat similar to the precursor MWCNTs but with a split extending longitudinally. Some MWCNTs are only partially split, remaining coiled at either end. The K-split MWCNTs retain their cylindrical shape because of strong interaction between the split walls. They resemble a rubber hose that is cut longitudinally but retains its cylindrical shape because of the thickness of the walls. The second type of conductive filler was prepared by the liquid-phase unzipping of MWCNTs with a potassium−sodium alloy.[21] The resulting stacked multilayered graphene nanoribbons (K/Na-unz GNRs) are predominantly unzipped and flattened (Figure 1c); they are not as rigid as K-split MWCNTs and can be easily bent at sharp angles. The third type of conductive filler was prepared by functionalization of K/Na-unz GNRs with iodohexadecane.[21] The resulting HD-GNR stacks are intercalated by hexadecane. In addition, hecadecyl alkyl groups are likely attached to the ribbon edges. This renders the HD-GNRs dispersible in organic solvents but simultaneously decreases their electrical conductivity. The appearance of HD-GNRs is very similar to that of K/Na-unz GNRs; they are predominantly unzipped and flattened. It is important to mention that all three types of GNRs used in this work have the same length because they are prepared from the same parent MWCNTs.

Because we have extensively characterized the GNRs earlier,[20,21] here we limit our discussion by pointing to the most relevant details. The Raman spectra (Figure 2a) show that the D band increases in the sequence MWCNT, K-split MWCNT, K/Na-unz GNR, and HD-GNR. In the Raman spectra of graphitic materials, the D band is activated by sp^3-hybridized carbon atoms present at edges and point defects or introduced by covalent basal plane functionalization. Apparently, in the case of the K-split MWCNT and K/Na-unz GNR, the D band is activated by the formation of additional edges during unzipping. In addition to the real microscopic edges of nanoribbon stacks, splitting/unzipping likely introduces some nanoscale edges, i.e., tiny cuts on the basal planes that do not result in visible microscopic cuts. Apparently, K/Na-unz GNRs have more cuts compared to the K-split MWCNTs, facilitating their flattening. Regarding HD-GNR, the large D band might arise not only from intercalation-related strain, as we suggested earlier,[21] but also from functionalization of graphene basal

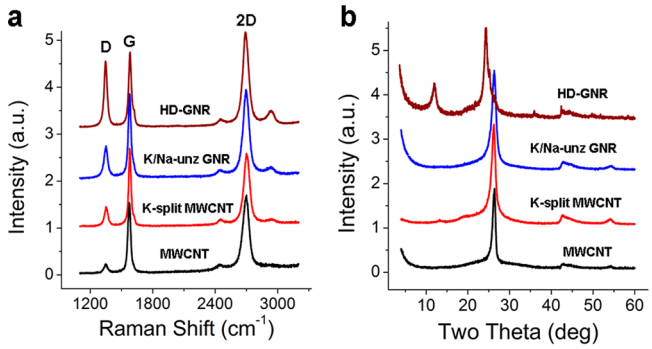

Figure 2. (a) Raman spectra and (b) XRD data for the four types of carbon nanostructures.

planes. X-ray diffraction (XRD; Figure 2b) shows the basic graphitic structure with the 002 signal at ~26.6° for K-split MWCNTs and K/Na-unz GNRs. In the case of HD-GNRs, XRD data indicate the formation of the stage-1 graphite intercalation compound.[21] Both covalent functionalization and intercalation make HD-GNRs less conductive compared to their counterpart K/Na-unz GNRs. Thus, the two types of GNRs have different conductivities with similar shapes, while K-split MWCNTs and K/Na-unz GNRs have similar conductivities but different shapes.

It was pointed out by several groups that the uniformity of the composite plays an important role in the electronic parameters.[14,16,17,22] Uniform distribution of all three types of conducting fillers was achieved in the NuSil matrix. The distribution of GNRs was analyzed by optical microscopy of thin layers of liquid uncured composite sandwiched between two microscope slides. We found that the GNR distribution changes little during the 15 min observation time. During the curing procedure, the composite immobilizes within the first 10 min after being placed in a drying oven. Thus, we conclude that in solid composites the GNR distribution is similar to that in the liquid form. Figure 3 shows optical microphotographs of composites with 0.5% filling fraction. One type of composite only is shown at each magnification scale because composites

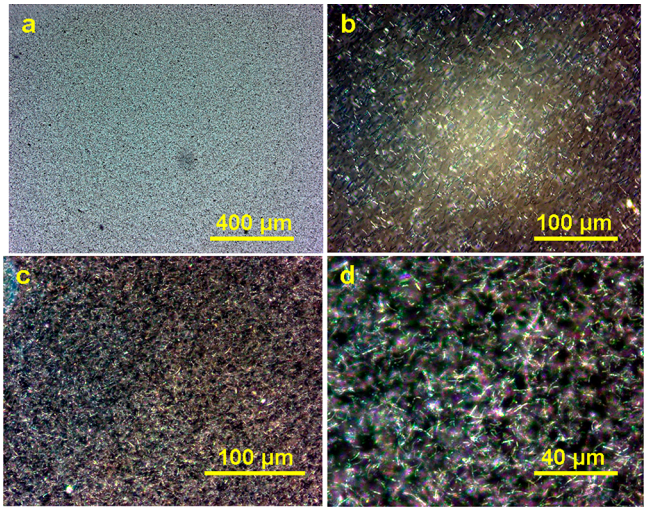

Figure 3. Optical microphotographs of thin films of composites: (a) K-split MWCNT/NuSil; transmitted light; (b) HD-GNR/NuSil; reflected light; (c and d) K/Na-unz GNR/NuSil; dark-field reflected light.

dx.doi.org/10.1021/am401859j | ACS Appl. Mater. Interfaces 2013, 5, 7567−7573

containing different inclusions look very similar. See the Supporting Information (SI) for more images. The low-magnification image (Figure 3a) demonstrates that the composite is uniform; only a few dark points of aggregates are visible. In the higher-magnification images (Figure 3b–d), one can distinguish single GNRs. The images demonstrate that the vast majority of GNRs are separate from each other; few aggregates were observed within the photograph frame. At 1.0% filling fraction, the aggregates make up ~3% of all of the filler. At 2.0% filling fraction, the number of aggregates is higher; observation is more difficult, but we did not detect any significant difference in the distribution of the three different types of filler. An observed difference is that the distribution of HD-GNRs is slightly more uniform and the distribution of K/Na-unz GNRs is slightly less uniform compared to the distribution of K-split MWCNTs (see the SI for details). The difference is likely not a primary contributor affecting the macroscopic differences in the composites.

In our previous report,[22] we showed that composites made with K-split MWCNTs exhibit lower dielectric constants compared to those made from the parent MWCNTs. We explained this phenomenon by the lower electrical conductivity of the former. Splitting induces numerous defects in the otherwise complete MWCNT structure; the conductivity decreases. No percolation threshold was observed at the relatively low filling fractions used in the previous study. In this work, we prepared and tested additional samples with higher filling fractions. The results are presented in Figure 4. The real permittivity is almost frequency-independent at low filling fractions (Figure 4a) and only slightly slopes in the frequency region 1–100 MHz. It is known that the permittivity of dielectric materials decreases with the frequency.[9−12] There is always a delay in the material's response to an applied alternating field, and at higher frequencies, the material is not completely polarized and relaxed. The experimental literature data vary widely, but in many studies, the change in the permittivity values occurs in the 10^4–10^7 Hz frequency region.[5,13,16] On the basis of these data, we conclude that sloped parts of the curves in the 1–100 MHz region (Figure 4a) are likely the higher-frequency part of the dramatic permittivity change region of 10^4–10^7 Hz. One can expect that, for frequencies <1 MHz, the permittivity values of the composites are significantly higher than those recorded at 1 MHz. By analyzing literature data, we conclude that the frequency range where the permittivity changes its value is not related to the size and shape of the conducting filler but depends mostly on the filling fraction. Thus, it is not polarization of a single CNT or GNR but interfacial interactions, or Maxwell–Wagner polarization, that is responsible for the phenomenon. As is evident from Figure 4a, the higher the filling fraction, the higher the frequency range where the dramatic permittivity change occurs.

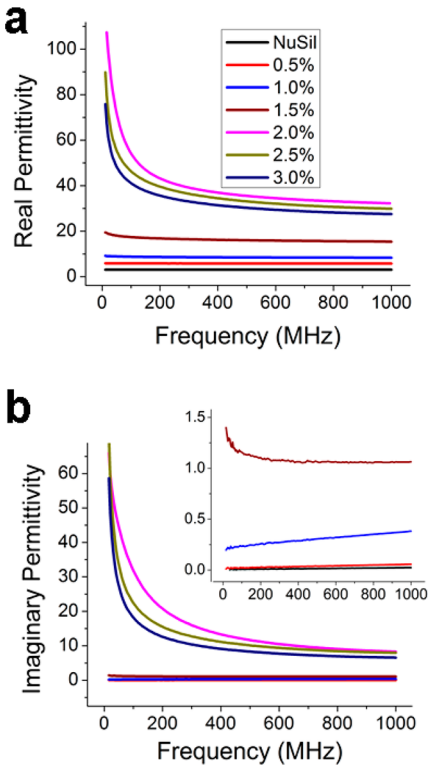

Figure 4. Frequency dependence of the (a) real and (b) imaginary parts of permittivity for K-split MWCNT/NuSil composites at different filling fractions. The inset in panel b is a Y-scale expansion in the 0–1.5 permittivity region.

The permittivity dependence on the loading fraction is almost linear at low (<1.0%) filling fractions. The permittivity sharply increases from 1.0% to 1.5% and especially from 1.5% to 2.0% filling fraction. After reaching a maximum at 2.0%, the permittivity insignificantly decreases with a further increase in the filling fraction (2.5% and 3.0%). The frequency dependence of the imaginary part (Figure 4b) is similar to that of the real part: the values are very low at 0.5–1.0%, and a sharp increase is observed between 1.0% and 2.0% filling fractions.

Fitting experimental results shown in Figure 4 with eq 2 indicates that both the proportionality coefficients and the critical exponents depend strongly on the filling fraction. All four parameters A, B, x, and y gradually increase from 0.5% to 1.5% filling fractions. Then they sharply increase from 1.5% to 2.0% and slowly decrease from 2.0% to 3.0%. Note that the imaginary permittivity plots (Figure 4b) for 0.5% and 1.0% filling fractions cannot be fitted by eq 2 because the imaginary part linearly increases with the frequency but does not exponentially decrease in accordance with eq 2. In general, both critical exponents x and y are within the 0.013–0.065 range for the 0.5–1.5% loaded samples. For the higher-loaded samples, exponent x decreases from 0.32 for the 2.0% sample to 0.23 for the 3.0% sample, while exponent y increases from 0.52 to 0.61, respectively. The loss tangent value calculated as B/A for the 1.5% loaded sample is 0.075, which is very close to the experimentally measured 0.070. For the higher filling fraction, the B/A values are generally 3–4 times higher than the experimentally determined loss values.

The electromagnetic behavior of K/Na-unz GNR/NuSil composites (Figure 5) was very different from that of K-split MWCNT/NuSil. First, the permittivity values were significantly higher. Thus, at 200 and 100 MHz, the real parts of the 2.5% composite were 411 and 729, respectively. To the best of our knowledge, such high permittivity values in the tested frequency region have never before been reported. For example, to achieve similar permittivity levels with MWCNT/epoxy composites, Wu and Kong[6] used a filling fraction of more than 23 wt %. Very high permittivity values were recently reported in the frequency region of 10–10^3 Hz.[16−18] The highest permittivity value in that region, reported by Dang et al.,[16] was ~6500 at 100 Hz for a composite comprising MWCNTs in a poly(vinylidene fluoride) (PVDF) host. At the

dx.doi.org/10.1021/am401859j | ACS Appl. Mater. Interfaces 2013, 5, 7567–7573

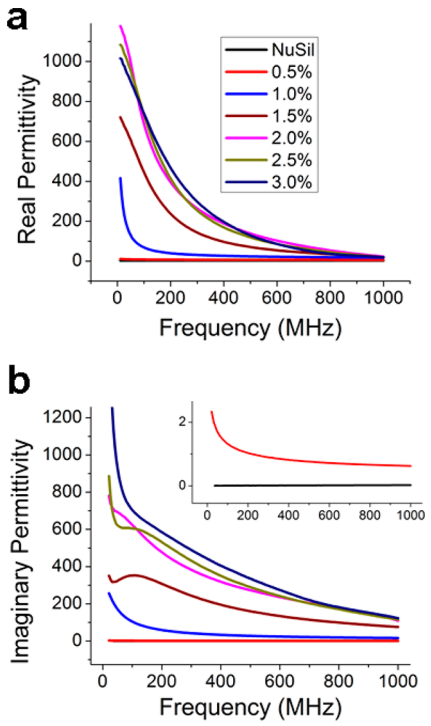

Figure 5. Frequency dependence of the (a) real and (b) imaginary parts of the permittivity for K/Na-unz GNR/NuSil composites at different filling fractions. The inset in panel b is a Y-scale expansion in the 0−2.0 permittivity region so that the NuSil and 0.5% lines can be differentiated; they overlap in the main graph.

same time, the permittivity level at 100 MHz was low, likely below 100, as one can estimate from the figure provided by the authors. We did not measure our composites at low frequencies, but in the 10−500 MHz region, the permittivity is significantly higher than those reported in the literature.[16−18] Note that Dang et al.[16] achieved high permittivity values by high filling fractions (15 vol %), while in our experiments, the filling fractions were almost 10-fold lower. Dang et al. attributed their high permittivity to specific interaction between the partially conductive PVDF and chemically modified MWCNTs. We do not suggest any specific interaction between the host and filler, and we explain the high dielectric constants by the uniform distribution and shape of the K/Na-unz GNRs.

Another peculiarity of the frequency-dependent curves (Figure 5a) is that permittivity values change in the entire tested frequency region, not only in the 10−100 MHz region, as they do for K-split MWCNT/NuSil (Figure 4a) and for CNT-comprising composites measured by the same impedance method.[4,8,22] Another distinctive characteristic of this type of composite is the extremely high value of the imaginary part (Figure 5b). At higher loading fractions (1.5−3.0%), the imaginary permittivity exceeds the real part in the 500−1000 MHz frequency region, which makes this type of composite extremely lossy. Critical exponents x and y are within the 0.81−0.99 and 0.71−0.75 regions, respectively, for all of the filling fractions except 0.5%, where the x and y values are 0.36 and 0.22, respectively. The high critical exponent values are expected from the shapes of the frequency-dependent curves (Figure 5a,b).

The control samples made from parent MWCNTs demonstrated that the real permittivity of K/Na-unz GNR/NuSil is higher than that of MWCNT/NuSil (Figure 6). This

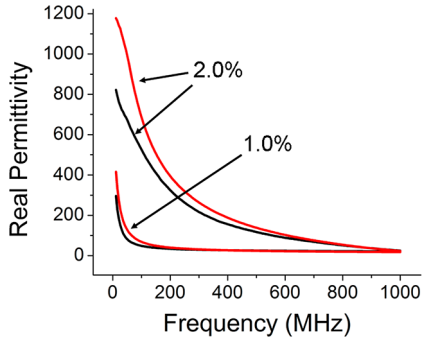

Figure 6. Real permittivity of composites containing K/Na-unz GNRs (red lines) versus composites containing parent MWCNTs (black lines) at two different filling fractions.

result is difficult to explain from the perspective of the conductivity of the inclusions. The conductivity of individual MWCNTs is significantly different,[23] but, on average, MWCNTs are more conductive than K/Na-unz GNRs. Apparently, the shape of K/Na-unz GNRs is what is responsible for the high dielectric constant values. The K/Na-unz GNRs are flat and have higher surface area. If one considers them as conducting plates of microcapacitors, then the higher plate area affords higher capacitance compared to their cylindrical K-split MWCNT counterparts. Alternatively, one can say that the larger volume of the dielectric host is effectively involved in building a microcapacitor network. The entire composite can accumulate more electrical charge, leading to higher interfacial polarization.

The permittivity of HD-GNR/NuSil composites (Figure 7) is significantly lower compared to that of K/Na-unz GNR/NuSil composites. The two fillers are similar in their

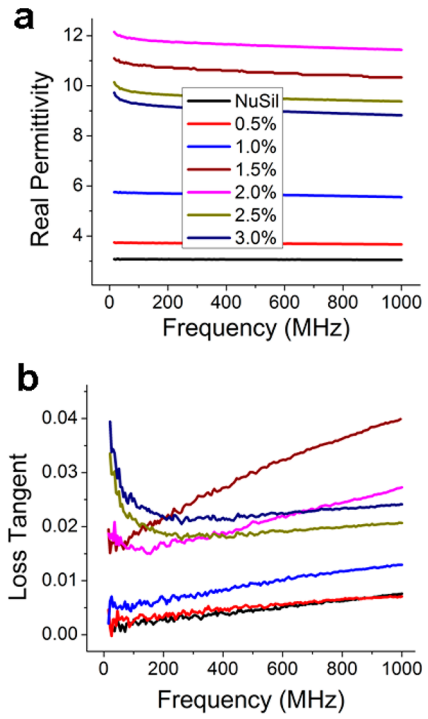

Figure 7. Frequency dependence of the (a) real permittivity and (b) loss tangent for HD-GNR/NuSil composites at different filling fractions.

dx.doi.org/10.1021/am401859j | ACS Appl. Mater. Interfaces 2013, 5, 7567−7573

geometrical parameters and differ only in their electrical conductivity, which is approximately 7 times lower for HD-GNR.[21] The real permittivity lines are almost flat in the entire region tested and only slightly change at frequencies <100 MHz (Figure 7a). The imaginary permittivities are low (not shown), which results in extremely low loss tangent values (Figure 7b). Thus, at the filling fractions 0.5% and 1.0%, the loss tangent does not exceed 0.005 and 0.011 in the entire tested region, being almost the same as that for the blank NuSil host. For higher loading fractions, the loss tangent is ~0.02, which is still a very low value. Thus, by incorporating HD-GNRs, we increased the permittivity of the dielectric host by a factor of 4 while maintaining the loss tangent at an ultralow level. Considering the light weight, flexibility, and excellent mechanical properties of the HD-GNR/NuSil composites, they will find numerous applications where low loss is critical.

Figure 8 shows the dielectric constant dependence on the filling fraction measured at 700 MHz. A clear maximum is

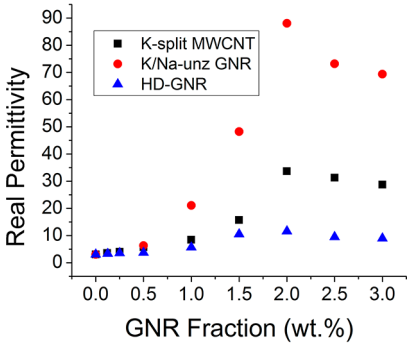

Figure 8. Variation of the real permittivity on the filling fraction for the three types of composite materials. The values were taken at 700 MHz.

detected at ~2.0% filling fraction for all three types of composites. The maximum for HD-GNR/NuSil is located between 1.5% and 2.0%, which can be attributed to the slightly better distribution of HD-GNRs in the polymer matrix. Experimental results shown in Figure 8 were fitted by eq 1, considering the measured maxima as "percolation threshold" values (f_c). To compare our results with literature data, we converted the weight percents that we used throughout the text into volume fractions (f). The density value of 2.11 g/cm^3 was used for all three types of carbon nanostructures (see the SI for details). The f_c values for K-split MWCNT/NuSil, K/Na-unz GNR/NuSil, and HD-GNR/NuSil were 0.00867, 0.00853, and 0.00796, respectively. The critical exponent (q) values were 1.02, 1.56, and 0.674, respectively. While the first number for q is almost equal to the universal one, the two others are significantly different. The obtained f_c values are significantly lower than most of the previously reported numbers for CNT/dielectric host composites (0.195,[4] 0.08,[14] 0.105,[16] and 0.066[17]). Only the work by Yao et al. reported similarly low threshold values.[24] We likely achieve low threshold values by very uniform distribution of GNRs in the host.

Despite the clear maximum of the dielectric constant observed at ~2.0% filling fraction (Figure 8), we are reluctant to consider it as a true percolation threshold. By definition, the percolation threshold is the fraction of a filler at which the inclusions form a continuous network. Such a continuous network of the conducting filler should inevitably render the composite conductive to direct electrical current. In our case, even at 3.0% loading, the samples did not show any detectable direct-current conductivity. From this perspective, the term "pseudothreshold" would be more appropriate.

The shape of the "permittivity vs filler fraction" curves is the subject of ongoing debate and research. According to eq 1, the curves should be symmetrical relative to the maximum value; the dielectric constant should equally increase by achieving the percolation threshold from either side. Realistically, the permittivity should not decrease after reaching the saturation maximum but remain near constant; the curves should be S-shaped.[25] Thus, in many experimental works, somewhat S-shaped curves were reported. However, significant permittivity decreases with increasing loading fraction were also reported.[16] In our work (Figure 8), the decrease in the permittivity from 2.0% to 3.0% loading fraction is not as significant as that in ref 16. It can be explained by partial aggregation, namely, conversion of microcapacitors into local direct-current conductive clusters. This results in a small decrease in the permittivity values, exactly as we detected. Thus, the region of a sharp increase in the permittivity from 1.0% to 2.0% filling fraction (Figure 8) is not a real percolation threshold. We define it as a "pre-threshold", the content of the conductive filler where the dielectric layer between the two adjacent filler particles, or microcapacitors plates, is the thinnest possible, providing the maximum capacitance value. When the filler fraction is further increased, the real percolation occurs locally and the macroscopic permittivity decreases. The nonsymmetrical character of the real curves (Figure 8) is additional evidence that the permittivity values are not governed by eq 1, and/or the explanation for the observed phenomena is outside that of percolation theory. From another perspective, there is no direct correlation between the direct-current conductivity and dielectric constant in general. A system might be non-direct-current-conductive even at extremely high fractions of the conductive filler. This can occur when the dielectric host has strong adsorption toward the conductive filler. A thin insulating layer of the polymer host on the surface of conductive filler particles will render the composite direct-current-nonconductive. Interfacial interaction of the two phases and subsequent Maxwell–Wagner polarization are the two factors that actually affect the dielectric constant of the composite materials. Ignoring these phenomena is a weak point of percolation theory in its application to the electromagnetic properties of dielectric composite materials. More realistic approaches are required to characterize these systems. As demonstrated by our experimental results, the microcapacitor model is a more realistic explanation of the electromagnetic properties of our dielectric composite materials.

CONCLUSION

We prepared new composite materials made by the incorporation of different of GNRs into a dielectric host matrix. By varying the type and content of the conductive filler, one can tune the loss and permittivity over a wide range of desirable values. The dielectric constant was tuned from moderate to extremely high values, while the corresponding loss tangent changed from ultralow to extremely high. The obtained data show that nanoscopic changes in the structure of the conductive filler can result in dramatic changes in the macroscopic properties of the composites. The microcapacitor model most realistically explains the behavior of our dielectric composites with the conductive filler.

■ ASSOCIATED CONTENT

Supporting Information

Uniformity of the conducting filler distribution in three different types of composites performed by optical microscopy (text and photographs). This material is available free of charge via the Internet at http://pubs.acs.org.

■ AUTHOR INFORMATION

Corresponding Author

*E-mail: kempel@egr.msu.edu (L.K.), rothwell@egr.msu.edu (E.J.R.), tour@rice.edu (J.M.T.).

Notes

The authors declare no competing financial interest.

■ ACKNOWLEDGMENTS

This work was supported by the AFOSR (FA9550-09-1-0581 and FA9550-09-1-0182), the Center of Excellence Low Carbon Technologies, Slovenia (CoE LCT), and the Center of Excellence Advanced Materials and Technologies for the Future, Slovenia (CoE NAMASTE). We thank Mitsui Inc. for the MWCNTs kindly supplied via Drs. M. Endo, A. Tanioka, and S. Tsuruoka. We thank C.-C. Hwang for the GNR density determination.

■ REFERENCES

(1) Baugham, R. H.; Zakhidov, A. A.; de Heer, W. A. *Science* **2002**, *297*, 787.
(2) Liu, Z.; Bai, G.; Huang, Y.; Li, F.; Ma, Y.; Guo, T.; He, X.; Lin, X.; Gao, H.; Chen, Y. *J. Appl. Phys.* **2007**, *111*, 13696.
(3) Shuba, M. V.; Slepyan, G. Y.; Maksimenko, S. A.; Hanson, G. W. *J. Appl. Phys.* **2010**, *108*, 114302.
(4) Grimes, C. A.; Mungle, C.; Kouzoudis, D.; Fang, S.; Eklund, P. C. *Chem. Phys. Lett.* **2000**, *319*, 460.
(5) Grimes, C. A.; Dickey, E. C.; Mungle, C.; Ong, K. G.; Qian, D. *J. Appl. Phys.* **2001**, *90*, 4134.
(6) Wu, J.; Kong, L. *Appl. Phys. Lett.* **2004**, *84*, 4956.
(7) Xiang, C.; Pan, Y.; Liu, X.; Sun, X.; Shi, X.; Guo, J. *Appl. Phys. Lett.* **2005**, *87*, 123103.
(8) Higginbotham, A.; Stephenson, J.; Smith, R.; Killips, D.; Kempel, L. C.; Tour, J. M. *J. Phys. Chem. C* **2007**, *111*, 17751.
(9) Laverghetta, T. *Microwave Materials and Fabrication Techniques*, 2nd ed.; Artech House: Boston, MA, 1991.
(10) Bergman, D. G.; Imry, Y. *Phys. Rev. Lett.* **1997**, *39*, 1222.
(11) Satuffer, D.; Aharony, A. *Introduction to Percolation Theory*, 2nd ed.; Taylor & Francis: London, 1998.
(12) Nan, C. W. *Prog. Mater. Sci.* **1993**, *37*, 1.
(13) Chen, Q.; Du, P.; Jin, L.; Weng, W.; Han, G. *Appl. Phys. Lett.* **2007**, *91*, 022912.
(14) Liu, L.; Matitsine, S.; Gan, Y. B.; Chen, L. F.; Kong, L. B.; Rozanov, K. N. *J. Appl. Phys.* **2007**, *101*, 094106.
(15) Chen, Q.; Du, P.; Jin, L.; Weng, W.; Han, G. *Appl. Phys. Lett.* **2007**, *91*, 022912.
(16) Dang, Z. M.; Wang, L.; Yin, Y.; Zhang, Q.; Lei, Q. Q. *Adv. Mater.* **2007**, *19*, 852.
(17) Yuan, J.-K.; Li, W.-L.; Yao, S.-H.; Lin, Y.-Q.; Sylvestre, A.; Bai, J. *Appl. Phys. Lett.* **2011**, *98*, 032901.
(18) Yuan, J.-K.; Yao, S.-H.; Dang, Z.-M.; Sylvestre, A.; Genestoux, M.; Bai, J. *J. Phys. Chem. C* **2011**, *115*, 5515.
(19) Dang, Z.-M.; Wu, J.-P.; Xu, H.-P.; Yao, S.-H.; Jiang, M.-J.; Bai, J. *Appl. Phys. Lett.* **2007**, *91*, 072912.
(20) Kosynkin, D. V.; Lu, W.; Sinitskii, A.; Pera, G.; Sun, Z.; Tour, J. M. *ACS Nano* **2011**, *5*, 968.
(21) Genorio, B.; Lu, W.; Dimiev, A. M.; Zhu, Y.; Raji, A.-R. O.; Novosel, B.; Alemany, L. B.; Tour, J. M. *ACS Nano* **2012**, *6*, 4231.
(22) Dimiev, A.; Lu, W.; Zeller, K.; Crowgey, B.; Kempel, L. C.; Tour, J. M. *ACS Appl. Mater. Interfaces* **2011**, *3*, 4657.
(23) Ebbesen, T. W.; Lezec, H. J.; Hiura, H.; Bennett, J. W.; Ghaemi, H. F.; Thio, T. *Nature* **1996**, *382*, 54.
(24) Yao, S.-H.; Dang, Z.-M.; Jiang, M.-J.; Xu, H.-P. *Appl. Phys. Lett.* **2007**, *91*, 212901.
(25) Grady, B. P. *Carbon Nanotube–Polymer Composites: Manufacture, Properties, and Applications*; Wiley: New York, 2011.